Spatiotemporal Analysis of Cardiac-Induced Thoracic Displacement Patterns Through High-Fidelity Modeling

Mohammadali Monfared[1], Amirtaha Taebi[1]

[1] Lehigh University, Bethlehem, PA, USA

Abstract

Cardiovascular diseases remain the leading cause of mortality worldwide, highlighting the need for improved monitoring and diagnosis techniques. While chest wall displacement reflects cardiac mechanical activity, conventional monitoring lacks the spatial resolution to characterize these displacements under various conditions. This study introduces a displacement-based finite element (FE) framework to simulate and analyze cardiac-induced chest wall motion using ECG-gated cardiac computed tomography data. Subject-specific cardiac motion was extracted via an optical flow algorithm and prescribed as a boundary condition to a thoracic FE model. This approach enables the computation of spatially resolved displacement across the chest surface. A 6×6 grid of uniformly distributed points is defined on the anterior chest surface for four healthy subjects, and displacement signals are analyzed over the cardiac cycle. The results reveal consistent spatiotemporal patterns of chest wall motion, with distinct propagation behavior aligned with key cardiac phases and strong correspondence to left ventricular volume dynamics. These results suggest that FE-based simulations can bridge the gap between internal cardiac mechanics and surface-level measurements, providing a physiologically interpretable foundation for next-generation non-invasive cardiac monitoring.

1. Introduction

Cardiovascular diseases remain the leading cause of death globally, accounting for up to 20 million deaths annually and 32% of all fatalities, with mortality rates resurging since 2019 [1,2]. This intensifying global burden highlights an urgent need for diagnostic paradigms that move beyond intermittent clinical visits. Consequently, there is a growing demand for cost-effective, non-invasive technologies capable of continuous, real-time monitoring of cardiac mechanical function.

Over the last decade, seismocardiography (SCG), gyrocardiography, and ballistocardiography have dominated the research landscape [3, 4], with SCG captures high-frequency chest wall vibrations via inertial sensors, though acceleration, being a second-order derivative of motion, is susceptible to noise and may obscure the underlying cardiac mechanics. In contrast, kinetocardiography (KCG) measures the low-frequency displacement of chest wall, offering a more direct physiologically interpretable representation of cardiac-induced motion, including changes in heart volume, shape, and position [5, 6]. Historically limited by instrumentation, KCG is now worth reconsidering thanks to advancements in sensing technologies and computational modeling.

While sensing technologies provide the raw data, clinical utility depends on accurately mapping surface vibrations back to internal cardiac events through the thorax which acts as a complex mechanical filter that attenuates and distorts the heart's signal. Computational modeling has emerged as a vital tool to "decode" this transfer function, bridging the gap between internal biomechanics and surface-level measurements. Recent SCG modeling efforts have begun to unravel this relationship, using finite element (FE) and image-driven frameworks to analyze how cardiac-induced vibrations propagate through the thorax [7, 8]. These studies have been instrumental in moving beyond empirical signal observation toward a deterministic understanding of signal genesis [8].

However, most modeling efforts to date have focused on the high-frequency acceleration components of SCG, which are inherently complex to interpret due to their sensitivity to sensor placement and tissue damping. While KCG offers a more direct, displacement-based alternative, yet it remains significantly underexplored in the computational domain.Early mathematical frameworks have demonstrated that simplified, sinusoidal assumptions of chest wall motion fail to capture the true complexity of thoracic dynamics [9]. There is a clear need for high-fidelity, physiologically realistic models that can simulate the full-field displacement of the chest. Such models would allow us to move beyond single-point measurements (which are prone to variability) toward a comprehensive spatiotemporal understanding of how the entire thoracic surface responds to the cardiac cycle.

Table 1. Material properties of thoracic tissues used in the computational model [8, 10].

Tissue type	Young's modulus	Density (kg/m^3)	Poisson's ratio
Chest muscle	2.5 MPa	1000	0.3
Ribcage	12 GPa	2000	0.4
Fat tissue	3.6 kPa	900	0.5
Lungs	4 kPa	600	0.45

This study addresses this gap by introducing a novel displacement-based FE framework that leverages ECG-gated computed tomography (CT) data to simulate cardiac-induced motion. By shifting the focus from point-based acceleration to spatially resolved displacement, we provide a more stable and physiologically interpretable representation of cardiac function. This approach not only enhances the fundamental understanding of the KCG signal but also establishes a computational foundation for next-generation, full-field non-invasive monitoring.

2. Materials and Methods

The proposed high-fidelity computational framework integrated cardiac CT, optical flow motion extraction, and FE modeling to simulate cardiac-induced thoracic displacement. The workflow began with the reconstruction of subject-specific thoracic geometries from ECG-gated CT data. Subject-specific cardiac wall motion was quantified via an optical flow algorithm and prescribed as a dynamic boundary condition to the FE model. The FE model was then used to simulate the spatiotemporal propagation and distribution of cardiac-induced motion.

2.1. Computational Domain

To create the computational domain, the anatomical geometry of the thorax, including the ribcage, lungs, and surrounding soft tissues, was reconstructed from cardiac CT data at the end-diastolic phase of three healthy adult subjects. In addition, cardiac wall motion was extracted from the time-resolved volumetric images using an optical flow algorithm, providing a spatially and temporally varying displacement field [8]. This algorithm was initialized by manually defining a set of points along the heart wall on the initial frame across multiple slices. A 3D Lucas–Kanade algorithm was then employed to track the motion of these points across consecutive volumetric frames throughout the cardiac cycle which finally resulted in time-resolved displacement vectors of the cardiac wall. The original ECG-gated CT datasets included 10 time frames for Subjects 1 and 2 and 20 time frames for Subject 3 over one cardiac cycle. To provide a consistent temporal input for the FE simulations, the extracted cardiac wall displacement fields were temporally interpolated to 120 Hz using cubic spline interpolation before being applied as displacement boundary conditions. Therefore, the simulated displacement maps were evaluated with a temporal spacing of approximately 8.3 ms over the normalized cardiac cycle. This subject-specific cardiac wall displacement field was used as the boundary condition in the FE simulations.

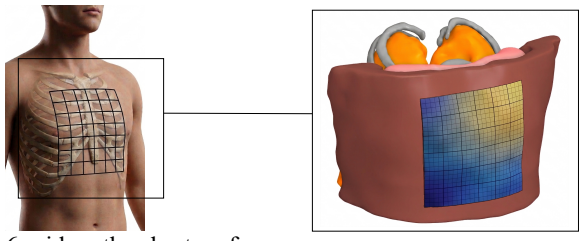

6x6 grid on the chest surface for displacement calculation

Extracted geometry for FEM simulation

Figure 1. Chest surface grid for displacement measurement and the corresponding computational domain. The contour on the chest surface shows the 6×6 grid displacement at a sample timestep during cardiac cycle.

2.2. Modeling Thoracic Displacements

An FE model of the thorax was constructed based on the reconstructed geometry. The mechanical behavior of tissues was modeled using homogeneous, isotropic, linear elastic material properties (Table 1). The simulations were performed as transient dynamic analyses, and damping was included using Rayleigh damping, in which the damping matrix was defined as ([C]=α[M]+β[K]). The computational domain was discretized using a tetrahedral mesh, and mesh convergence and time dependence analysis was performed to ensure solution independence from element size and timestep. Detailed computational settings were reported in our previous work [8]. By applying the prescribed displacement boundary condition on the cardiac surface, the mechanical response of the surrounding structures was simulated, governed by the equation of motion:

$$[M]\{\ddot{q}\} + [C]\{\dot{q}\} + [K](\{q\} - \{u\}) = \{f(t)\} \quad (1)$$

where $[M]$, $[C]$, and $[K]$ denote the mass, damping, and stiffness matrices, respectively, $\{u\}$ represents the prescribed cardiac motion, $\{q\}$ is the resulting displacement field of the thoracic structures, and $\{f(t)\}$ is the applied force vector. Unlike previous studies that primarily focused on acceleration-based signals, the present work emphasizes direct analysis of chest wall displacement. First, a region of interest (ROI) on the anterior chest surface was defined, bounded laterally by the left and right nipples, superiorly by the top of the sternum, and inferiorly by the xiphoid process. The ROI was discretized into a 6×6 grid,

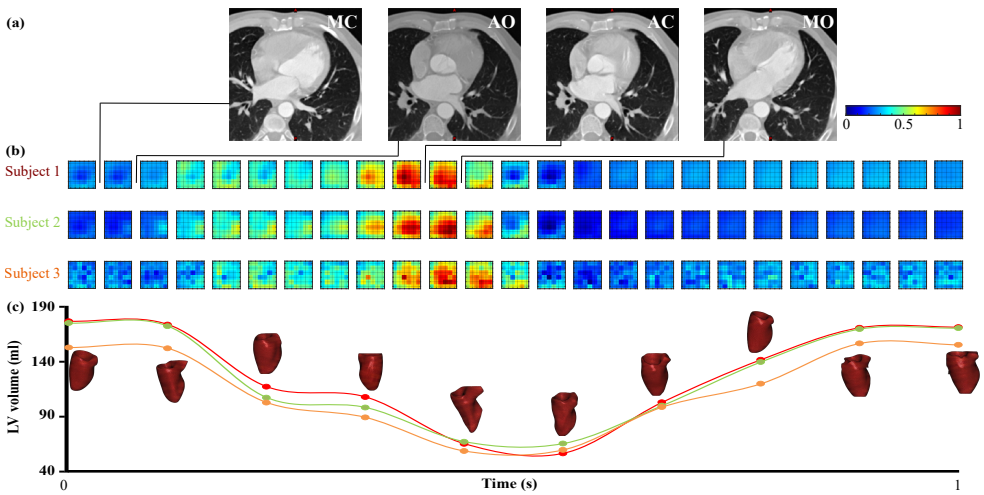

Figure 2. (a) Representative cardiac events identified from caqrdiac CT images, including mitral valve closure (MC), aortic valve opening (AO), aortic valve closure (AC), and mitral valve opening (MO). Temporal alignment between the CT-derived cardiac events and the simulated displacement maps was established by estimating the occurrence time of fiducial points from the CT data. (b) Time-resolved, spatially distributed chest wall displacement maps for three subjects, computed over one cardiac cycle on a 6×6 grid covering the anterior thoracic surface. The displacement values are normalized between 0 and 1 to facilitate inter-subject comparison. (c) Left ventricular (LV) volume variation for the three subjects.

resulting in 36 uniformly distributed points on the chest surface. The center of each grid cell was considered as a representative point, and the displacement of these points was tracked over the cardiac cycle. Figure 1 illustrates, for a representative subject, the spatial distribution of the selected points along with the corresponding FE thoracic geometry. The simulated displacement maps were analyzed in spatial and temporal domains to characterize the propagation of cardiac-induced motion across the chest surface.

3. Results

In this study, three sets of cardiac CT scan data were utilized to evaluate spatiotemporal variations of cardiac-induced chest displacement. For each subject, displacement fields were computed over the cardiac cycle using the proposed finite element framework that enable analysis of spatially distributed motion patterns across the anterior chest surface. The displacement signals were extracted at predefined grid points within the ROI and provide a consistent basis for comparing temporal evolution and spatial distribution of chest wall motion across subjects 1.

Figure 2 presents the spatiotemporal distribution of cardiac-induced chest wall displacement across three subjects. As shown in Fig. 2(a), key cardiac events identified from the CT data, including mitral valve closure (MC), aortic valve opening (AO), aortic valve closure (AC), and mitral valve opening (MO) points, are temporally aligned with the simulated displacement maps obtained from the FE model. This alignment establishes a direct correspondence between physiological cardiac events and their manifestation in the measurable body surface signals.

Table 2. Quantitative summary of simulated chest wall displacement over the 6×6 grid. Values are reported as absolute displacement magnitudes in millimeters.

Subject	Max. disp. (mm)	Mean point-wise peak disp. (mm)	Peak spatial mean disp. (mm)
Subject 1	0.803	0.544	0.503
Subject 2	0.808	0.223	0.216
Subject 3	1.390	0.883	0.790

In addition to normalized displacement maps, the maximum simulated chest wall displacement are reported in Table 2 and ranged from 0.803 to 1.390 mm across the three subjects. These values indicate that the simulated chest wall motions were in a measurable range and provide quantitative support for the sensing feasibility of spatial displacement-based cardiomechanical monitoring.

Temporal analysis of the normalized displacement fields reveals a consistent propagation pattern strictly tied to distinct cardiac phases. As illustrated in Fig. 2(b), minimal chest wall displacement is observed at the onset of systole (MC). However, displacement magnitude increases significantly during the ventricular ejection phase, between AO and AC. Peak outward displacement (indicated by the maximum intensity zones) is consistently reached immediately prior to and at the point of AC across all subjects. Notably, this peak surface displacement occurs inversely to the left ventricular volume, which reaches its minimum at end-systole. This phenomenon perfectly captures the

complex three-dimensional kinematics of the heart; during forceful systolic contraction, the anterior rotational thrust of the myocardium, clinically recognized as the apical impulse, exerts maximum outward force against the thoracic boundary despite the overall reduction in internal cardiac volume. Following AC, the displacement rapidly attenuates through the isovolumic relaxation phase prior to MO, as the ventricles recoil and internal pressures drop. These findings demonstrate that the proposed FE framework accurately translates complex internal structural kinematics, such as rotational and translational myocardial shifts, into physiologically realistic surface displacement, moving beyond simple volumetric correlation.

Beyond temporal alignment, analyzing the full 6×6 grid highlights critical inter-subject variability in the spatial distribution of the displacement. As seen in Fig. 2(b), Subjects 1 and 2 exhibit a highly localized "epicenter" of outward motion during the ejection phase. This focal point (likely corresponding to the anatomical projection of the cardiac apex) creates a clean, radiating displacement pattern. Conversely, while Subject 3 follows the identical temporal trajectory (reaching maximum displacement at AC), the spatial signature is noticeably more diffuse and distributed across the thoracic surface. This variance is expected in physiologically realistic models and can be attributed to underlying anatomical differences, such as variations in chest wall thickness, rib orientation, tissue mechanics, and the geometric distance between the myocardium and the sternum. Crucially, this variation underscores the inherent limitation of conventional single-point sensing modalities; a single sensor placed at a standardized location might accurately capture the peak mechanics of Subjects 1 and 2 but could completely miss the true epicenter of motion for Subject 3. By providing spatially resolved, full-field displacement maps, this FE framework demonstrates the necessity of array-based analysis to accurately characterize cardiomechanical activity across diverse patient anatomies. Finally, this displacement-based analysis enabled a more direct and physiologically interpretable assessment of thoracic mechanical response compared to acceleration-derived signals. They allowed direct observation of regional deformation and motion propagation across the chest surface, which cannot be easily inferred from acceleration signals alone.

4. Conclusion

This study presents a novel modeling framework driven by CT data to simulate spatially resolved cardiac-induced chest wall displacement. Results demonstrate that peak outward displacement consistently occurs during ventricular ejection, accurately capturing the apical impulse. Additionally, spatial variability in the motion's epicenter across subjects underscores the limitations of single-point sensors, validating the need for array-based approaches. Ultimately, this high-fidelity model provides a physiologically interpretable foundation for advancing next-generation, non-invasive cardiomechanical monitoring.

Acknowledgments

This work was supported by the U.S. National Science Foundation (Grant No. 2340020 and 2618456).

References

[1] Baghdadi NA, Farghaly Abdelaliem SM, Malki A, Gad I, Ewis A, Atlam E. Advanced machine learning techniques for cardiovascular disease early detection and diagnosis. Journal of Big Data 2023;10(1):144.

[2] Woodruff RC, Tong X, Khan SS, Shah NS, Jackson SL, Loustalot F, Vaughan AS. Trends in cardiovascular disease mortality rates and excess deaths, 2010–2022. American journal of preventive medicine 2024;66(4):582–589.

[3] Taebi A, Solar BE, Bomar AJ, Sandler RH, Mansy HA. Recent advances in seismocardiography. Vibration 2019; 2(1):64–86.

[4] Inan OT, Migeotte PF, Park KS, Etemadi M, Tavakolian K, Casanella R, Zanetti J, Tank J, Funtova I, Prisk GK, et al. Ballistocardiography and seismocardiography: A review of recent advances. IEEE journal of biomedical and health informatics 2014;19(4):1414–1427.

[5] Eddleman Jr E. Kinetocardiographic changes in ischemic heart disease. Circulation 1965;32(4):650–655.

[6] Schweizer W, Bertrab R, Reist P. Kinetocardiography in coronary artery disease. British Heart Journal 1965; 27(2):263.

[7] Monfared M, Thibbotuwawa Gamage P, Taebi A. Investigating seismocardiogram patterns: A computational modeling of cardiac wall motion propagation to the chest surface. In ASME International Mechanical Engineering Congress and Exposition, volume 88629. American Society of Mechanical Engineers, 2024; V004T06A006.

[8] Monfared M, Kakavand B, Gamage PT, Taebi A. Digital twin-based investigation of seismocardiogram sensitivity to tissue mechanics and myocardial motion. Journal of Biomechanical Engineering 2025;147(12):121007.

[9] Singh A, Rehman SU, Yongchareon S, Chong PHJ. Modelling of chest wall motion for cardiorespiratory activity for radar-based ncvs systems. Sensors 2020;20(18):5094.

[10] Gamage PPT. Seismocardiography-genesis, and utilization of machine learning for variability reduction and improved cardiac health monitoring. Ph.D. thesis, University of Central Florida, 2020.

Address for correspondence:

Amirtahà Taebi

Department of Bioengineering, Lehigh University, Bethlehem, PA 18015, USA

e-mail: amirtaha@lehigh.edu